Published in final edited form as:
Plant J. 2013 November ; 76(4): 592–602. doi:10.1111/tpj.12318.

Regulation of cell divisions and differentiation by MALE STERILITY32 is required for anther development in maize

Jihyun Moon[1], **David Skibbe**[2], **Ljudmilla Timofejeva**[1,3], **Chung-Ju Rachel Wang**[4], **Timothy Kelliher**[2], **Karl Kremling**[1], **Virginia Walbot**[2], and **William Zacheus Cande**[1,*]

[1]Department of Molecular and Cell Biology, University of California at Berkeley, Berkeley, CA 94720, USA

[2]Department of Biology, Stanford University, Stanford, CA 94305, USA

[3]Department of Gene Technology, Tallinn University of Technology, Tallinn 12618, Estonia

[4]Institute of Plant and Microbial Biology, Academia Sinica, Taipei 11529, Taiwan

Summary

Male fertility in flowering plants relies on proper division and differentiation of cells in the anther, a process that gives rise to four somatic layers surrounding central germinal cells. The maize gene *male sterility32* (*ms32*) encodes a basic helix–loop–helix (bHLH) transcription factor, which functions as an important regulator of both division and differentiation during anther development. After the four somatic cell layers are generated properly through successive periclinal divisions, in the *ms32* mutant, tapetal precursor cells fail to differentiate, and, instead, undergo additional periclinal divisions to form extra layers of cells. These cells become vacuolated and expand, and lead to failure in pollen mother cell development. *ms32* expression is specific to the pre-meiotic anthers and is distributed initially broadly in the four lobes, but as the anther develops, its expression becomes restricted to the innermost somatic layer, the tapetum. The *ms32-ref mac1-1* double mutant is unable to form tapetal precursors and also exhibits excessive somatic proliferation leading to numerous, disorganized cell layers, suggesting a synergistic interaction between *ms32* and *mac1*. Altogether, our results show that MS32 is a major regulator in maize anther development that promotes tapetum differentiation and inhibits periclinal division once a tapetal cell is specified.

Keywords

anther development; cell division; differentiation; maize; bHLH; cytology

Introduction

In plants, germ cells arise *de novo* from somatic cells late in development during the reproductive phase of development. This process differs from that of animals, which form

*For correspondence (zcande@berkeley.edu).

Supporting Information: Additional Supporting Information may be found in the online version of this article.

germ-line stem cells during embryogenesis. The switch from vegetative to reproductive phase in plants occurs as the shoot apical meristem stops producing vegetative organs, such as leaves, stems, and lateral buds, and becomes an inflorescence meristem, which produces floral meristems. During the development of male and female reproductive organs, germinal cells competent for meiosis then differentiate from subepidermal somatic cells in the anther and ovule.

In maize, each male floret contains three anthers (Figure 1a) that develop into a four-lobed structure that contains central germinal cells in each lobe surrounded by a somatic niche (Figure 1b). Mosaic analysis with maize anthers has shown that both epidermal (L1) and inner (L2) layer cells of the meristem contribute to the formation of anthers (Dawe and Freeling, 1990). As an attempt to explain how pre-meiotic germinal cells, called archesporial cells, arise *de novo* from this population of somatic cells, cell lineage models proposed that a L2-derived hypodermal cell undergoes a single periclinal division to generate an inner archesporial cell and an outer somatic (primary parietal) cell (Ma, 2005). Recently, using confocal microscopic analysis on maize anthers, new observations were made on the process of archesporial cell formation in maize (Kelliher and Walbot, 2011). Instead of well defined hypodermal cells that undergo periclinal divisions, L2-derived cells were observed in a disorganized manner encircled by the epidermis. Without any significantly notable asymmetric divisions, archesporial cells were shown to arise in the center of a group of approximately 100 L2-derived cells.

Many anther development mutants have been isolated in maize in male sterility screens, in which female fertility is usually unperturbed. In the *male sterile converted anther1* (*msca1*) mutant, archesporial cells are missing and somatic cells acquire a leaf cell-like fate (Chaubal *et al.*, 2003). *msca1* encodes a glutaredoxin, which acts as a redox regulator of a target proteins, which may include transcription factors (Albertsen *et al.*, 2011). Interestingly, a reductive environment applied to *msca1* anthers was shown to rescue archesporial cell formation, this finding suggests that hypoxia in the center of the lobes triggers archesporial cell specification via MSCA1 (Kelliher and Walbot, 2012). The *multiple archesporial cells1* (*mac1*) mutant has an excess number of archesporial cells but a limited number of somatic cells (Sheridan *et al.*, 1999). Recent cloning of the gene has shown that *mac1* encodes a small secreted protein (Wang *et al.*, 2012), which is the ortholog of rice TAPETUM DETERMINANT-LIKE1A (TDL1A; Zhao *et al.*, 2008). TDL1A has been shown to act as a ligand of the leucine rich repeat receptor-like kinase MULTIPLE SPOROCYTES1 (MSP1; Nonomura *et al.*, 2003; Zhao *et al.*, 2008). Several maize mutants with defects limited to somatic layer differentiation have also been identified. One example is the mutation in the HD-ZIP IV gene *outer cell layer4* (*ocl4*). In *ocl4*, an extra subepidermal layer with endothecium characteristics is observed, which spatially coincides with the specific expression of the gene in the epidermis of normal anthers (Vernoud *et al.*, 2009). Coordinate expression of MAC1 and OCL4 establishes conditions that allow precisely one periclinal division by the L2-derived somatic cells between the epidermis and the newly formed archesporial cells.

Despite the large collection of male sterile mutants in maize, only a few mutants have been studied in detail. Recently, many uncharacterized and several newly isolated mutants have

been classified into several categories based on their cytological phenotypes and several new alleles of known mutants have been isolated (Timofejeva *et al.*, 2013). The *male sterility32* (*ms32*) mutant is noteworthy because of extra periclinal divisions in the L2-cell layer and excessive elongation of the novel cell types that crush the sporogenous cells at maturity (Chaubal *et al.*, 2000; Timofejeva *et al.*, 2013). Here, we report the cytological characterization of the *ms32* mutant phenotype. Additional periclinal divisions initiate during pre-meiotic anther development after all four somatic layers are established. Molecular cloning has demonstrated that *ms32* encodes a basic helix–loop–helix (bHLH) transcription factor that is orthologous to rice UNDEVELOPED TAPETUM1 (UDT1; Jung *et al.*, 2005), but phenotypically distinct from the *udt1* mutant. The expression of *ms32* is restricted temporally to pre-meiotic anther development, with broad expression across cell types in the early stages and spatially refined, tapetum-specific expression at later stages. Our results suggest that the role of MS32 is to suppress periclinal cell division in the tapetal cells after their anticlinal cell divisions have ceased and to foster, directly or indirectly, proper tapetal cell differentiation to support meiocytes.

Results

Allelism test establishes two alleles of *ms32*

The original maize *ms32* mutant has additional somatic layers in the anther, this situation results in male sterility (Figure 1d; Chaubal *et al.*, 2000). Extensive allelism testing during a characterization of hundreds of maize male sterile mutants demonstrated that an independently isolated mutant, known as *ms*-6066*, was allelic to the original *ms32* mutant (Timofejeva *et al.*, 2013). Both alleles of *ms32* showed extra periclinal divisions and defects in tapetal layer differentiation. We designated the original allele as *ms32-ref* and *ms*-6066* as *ms32-6066*.

ms32 regulates cell division and differentiation of the tapetal and middle layers

To understand the defect in *ms32-ref*, the cytology of wild-type and *ms32-ref* anthers were compared by analysis of semi-thin transverse sections. Early in anther development, each lobe consists of a single epidermal layer and a small mass of internal somatic cells, the pluripotent L2-d cells (also referred to as L2-derived cells). After germinal cells are specified, the surrounding subepidermal layer undergoes a single periclinal division that results in three somatic layers (Figures 1b and 2a). The subepidermal layer differentiates into the endothecium while the inner secondary parietal layer undergoes another round of periclinal division (Figures 1b and 2b,c), to generate four somatic layers in the anther. After this last periclinal division, the innermost layer that surrounds the archesporial cells becomes the tapetum, while the layer in between the tapetum and the endothecium differentiates into the middle layer (Figures 1b,c and 2c,d).

Anthers of *ms32-ref* cannot be distinguished from that of fertile siblings until the four somatic layers have been established (Figure 2e,f). Prior to the visible defect in *ms32*, enlarged, differentiated archesporial cells are positioned at the center of each lobe, with small, cuboidal secondary parietal cells surrounding them. The endothecium layer also seems to differentiate properly with typical cell size and elongated width. In contrast with

wild-type, in which a single division in every secondary parietal cell over a narrow window of time results in the middle layer and tapetal precursors (Figure 2b,c), extra divisions occur in both layers in *ms32-ref* (Figures 2g,h and S1). These extra divisions do not happen simultaneously throughout the entire layer but occur gradually as the anther expands its volume through anticlinal divisions. In addition, these divisions occur predominantly in the tapetal precursors, infrequently in the middle layer and, rarely, in the endothecium (Figure S1). As the mutant anther matures, the multi-layered tapetal precursors become vacuolated and elongated, which in turn crush the microsporocytes at the center of the locule (Figure 1d). These observations suggest that normal *ms32* function is required to prevent periclinal divisions in the middle and tapetal layers and to ensure proper tapetal differentiation once the precursors are established.

ms32 encodes a bHLH protein

The *ms32-ref* mutation was placed initially distal to the UNC139 marker on chromosome 2 by bulked segregant analysis (Chaubal *et al.*, 2000). Using a population of 249 male sterile individuals, the *ms32* gene was mapped to an interval of 0.5 Mb (Figure 3a). Among the 15 genes in this region, the *ms32-ref* mutant was found to carry a >1.6 kb deletion in the GRMZM2G163233 gene model (Figure 3b).

The GRMZM2G163233 spans approximately 10 kb and contains four annotated transcript types, which included one transcript that has similarity to the N-terminal domain of a bHLH protein and a C-terminal vacuolar ATP synthase subunit H (Figure S2). Using CoGe (Lyons and Freeling, 2008; Lyons *et al.*, 2008), syntenic regions in the rice, *Brachypodium* and *Sorghum* genomes were compared with this maize genomic region. In all three genomes, the bHLH gene and the vacuolar ATP synthase subunit H gene were annotated as separate genes (Figure S3). As our attempt to amplify the mRNA across this whole predicted gene model failed, we explored expression-based evidence to determine if GRMZM2G163233 is actually two genes. Among the four annotated transcripts, only GRMZM2G163233_T01 encompasses both the bHLH domain and the vacuolar ATPase subunit. GRMZM2G163233_T02 and GRMZM2G16 3233_T03 correspond to the bHLH domain while GRM ZM2G163233_T04 corresponds to the vacuolar ATP synthase subunit (www.maizegdb.org). The EST sequences and PlantGDB-assembled unique transcripts aligned to GRMZM2G163233 cluster to either GRMZM2G163233_T02/T03 or GRMZM2G163233_T04, but none spanned all transcripts as predicted in GRMZM2G163233_T01 (Figure S2). Taken together, this finding strongly suggested that GRMZM2G163233 is a chimera of two genes, one of which is *ms32*.

The deletion in *ms32-ref* was confirmed to include the C-terminal half of the bHLH gene; however, the 3′ end of the deletion could not be identified (Figure 3b). Additional evidence that the bHLH gene is *ms32* was provided by examination of two Uniform*Mu* insertions lines (Settles *et al.*, 2007; McCarty and Meeley, 2009). The line *mu1043594::Mu* contains a *Mu* insertion in the second exon of the region that encodes the bHLH protein and that corresponds to transcripts GRMZM2G163233_T02/T03; the line *mu1019067::Mu* contains a *Mu* insertion in a region that encodes ATP synthase subunit H protein, which corresponds to the first exon in transcript GRMZM2G163233_T04 (Figure S2). The line

mu1019067::Mu did not show any sterility while *mu1043594::Mu* showed male sterility. Sterile *mu1043594::Mu* plants were crossed by *ms32-ref/+* and half of the progeny showed male sterility. This non-complementation supports the conclusion that *mu1043594::Mu* is an allele of *ms32*, and that the GRMZM2G163233_T02 transcript model corresponds to the *ms32* gene. The fertile phenotype of *mu1019067::Mu* suggests that the vacuolar ATP synthase does not play a role in anther development and provides strong evidence that GRMZM2G163233 is mis-annotated, and presents two individual genes. Thus, from this point on, we will consider GRMZM2G163233 to be two genes: GRMZM2G163233_T02 as the *ms32* gene that encodes the bHLH protein and GRMZM2G163233_T04 as the vacuolar ATP synthase subunit H gene (Figure S2).

The candidate gene (GRMZM2G163233_T02) consists of four exons that are predicted to encode a 219 amino acid protein (Figure 3b). The deletion in *ms32-ref* begins immediately after the second exon and extends beyond exon 4, thus leaving the N-terminal bHLH domain intact (Figure 3b). Full-length transcripts of the bHLH gene failed to amplify in *ms32-ref* due to the deletion (Figure 3c). The remaining N-terminal region of this gene (exons 1 and, 2) was still expressed in *ms32-ref* (Figure 3d). Interestingly, the N-terminal region expression level was higher in *ms32-ref* than the corresponding region of the functional allele in the wild-type siblings, a finding that suggests a possible regulatory unit in the C-terminus of the gene. Otherwise, the deletion could have brought an ectopic regulatory unit close to the remaining *ms32* gene, which is normally not part of the *cis*-elements of *ms32*. qRT-PCR using primers specific to the deleted region showed the lack of expression, and confirmed the deletion in *ms32-ref* (Figure 3d).

In the independently isolated *ms32-6066* allele, a *ruq*-transposon insertion was found in the first intron of the candidate gene (Figure 3b). The size and expression level of the mRNA in *ms32-6066* did not differ noticeably from the wild-type (Figure 3c), but six additional nucleotides were found in the mRNA sequence (Figure 3b). PCR amplification and sequencing of the first intron in *ms32-6066* showed that approximately 70 bp of the intron sequence was deleted and replaced by the *ruq*-transposon and the six additional nucleotides in the mRNA sequence originated at the junction of intron 1 with exon 2 and exon 3, a finding that suggested that the *ruq*-transposon may interfere with splicing of the *ms32-6066* transcript (Figure 3b). Unlike most insertions, which result in a frame shift in the protein sequence, these six nucleotides add two amino acids, valine (V) and glutamine (Q) at position 81 in frame with the predicted protein (Figure 3b). This insertion is within the bHLH domain thus suggesting that the mutant protein is non-functional; the bHLH domain contributes to DNA binding and/or interaction with other proteins, and we hypothesize that one or both of these processes are impaired in the MS32-6066 protein.

Syntenic analysis between maize and rice suggested that the *ms32* gene is an ortholog of the rice *UDT1* gene (Figure S3), which has been shown to be required in rice anther ontogeny (Jung *et al.*, 2005). Pairwise alignment of MS32 protein with UDT1 showed 72.2% identity at the amino acid level (Figure S4). Analysis of the bHLH domain in MS32 showed that all residues that are important for DNA binding and/or interaction with other proteins are conserved in maize and rice (Figure S4).

ms32 expression is specific to the pre-meiotic anther

To further understand the function of *ms32* during anther development, *ms32* expression was analyzed in pre-meiotic, meiotic, and post-meiotic anthers and in leaves. qRT-PCR demonstrated that *ms32* is restricted temporally to pre-meiotic anthers (Figure 3e), which coincides with the mutant phenotype that occurs during pre-meiotic anther wall development.

Spatiotemporal expression of *ms32* was analyzed by *in situ* hybridization. In young anthers that have just finished specifying the archesporial cells, *ms32* expression appears broadly in the L2-derived cells in each lobe and also in the presumptive central vasculature (Figure 4a,b). As anther development proceeds, the expression pattern of *ms32* becomes more refined, first by excluding expression in the endothecium (Figure 4c). By the four somatic cell layer stage, *ms32* expression was restricted spatially to only the tapetal layer (Figure 4d,e). Low expression was observed in the archesporial cells and pollen mother cells but never observed in the epidermis (Figure 4b–e). No specific expression was observed in *ms32-ref*, a result that indicated that the probe was specific (Figure 4f). This spatiotemporal specificity in expression agrees well with the suggested *ms32* role in periclinal division control and in modulation of tapetum differentiation.

The functional relationship between *ms32* and *mac1*

In the *mac1-1* mutant, excess archesporial cells are specified early in anther development, and they overproliferate while periclinal divisions in adjacent somatic layers are severely reduced (Sheridan *et al.*, 1999; Wang *et al.*, 2012). The middle layer and the tapetum are never defined in the *mac1-1* mutant, a result that indicated that the initial periclinal division is required to establish the secondary parietal layer and its subsequent periclinal division are a prerequisite for promoting those cell fates. The MAC1 protein localizes to archesporial cells and is a secreted ligand, which coincides with its function as a master regulator of periclinal divisions, which derived from an archesporial cell source. In *ms32-ref*, the normal, programmed periclinal divisions occur normally, but once tapetal precursors are born they do not differentiate properly; instead additional periclinal divisions occur in tapetal precursors and the cells misdifferentiate. In addition to opposing functional roles, *ms32* expression (Figure 4) overlaps with the localization of MAC1 protein, a result that suggested a possibility of functional interaction between the two proteins.

To further understand the genetic relationship between *ms32-ref* and *mac1-1*, double mutants were generated and analyzed. In early anther development, *ms32-ref mac1-1* resembles *mac1-1* with overproliferated archesporial cells (Figure 5c,d). Some L2-derived cells of *ms32-ref mac1-1* undergo a periclinal division as in wild-type or *ms32-ref*, but the majority of the cells remains as a single layer as in *mac1-1* (Figure 5b,d). This phenotype suggests that periclinal cell division in the L2-derived layer can be promoted even in the absence of functional MAC1 and that MS32 is involved in suppression of this process as well. As the wild-type and *ms32-ref* siblings reach the four-layer stage, both *mac1* and *ms32-ref mac1-1* anthers show undeterminated somatic cells that surround the pollen mother cells (Figure 5g,h). Due to the *ms32-ref* mutation, the *ms32-ref mac1-1* anthers showed additional divisions compared with *mac1-1* (Figure 5g,h). These divisions were not oriented

periclinally as is observed in *ms32-ref* single mutants, but occurred in a disorganized manner as in *mac1-1*. In addition, the cells were smaller in the double mutant, a situation that suggested that the *ms32-ref* mutation promotes the division rate and leads to failure in cell growth. What drives these divisions in later stage *mac1-1* and *ms32-ref mac1-1* anthers is still unknown. However, the additive phenotype in the double mutant suggests that MS32 has a function even after late anther development to control divisions in these somatic cells.

The relationship between the two genes was further characterized by pairwise qRT-PCR in RNA from mixed stage anthers. *ms32* expression is upregulated in *mac1-1* (Figure 6a), and suggested two possibilities: (i) either MAC1 is a negative regulator of *ms32* expression; or (ii) the undifferentiated cells in *mac1-1* contribute to the higher level of *ms32* expression. The proportion of the undifferentiated somatic cells in *mac1-1* anthers would be much higher than that of the secondary parietal layer and tapetum in wild-type anthers, which could result in higher levels of *ms32* that has a broad expression throughout the L2-derived cells (Figure 4a,b). In addition, it is less likely that MAC1 is a major negative regulator of *ms32* considering that *ms32* expression overlaps in the somatic layers where MAC1 exists and that *ms32-ref mac1-1* double mutants show an additive phenotype (Figure 5). However, to our surprise, *mac1* expression is decreased in *ms32-ref* relative to that in wild-type suggesting that functional MS32 is required for normal *mac1* expression (Figure 6b). This situation could also be due to the aberrant anther development in *ms32-ref*, as the male sporocytes, which normally express MAC1, have collapsed as the tapetal precursors undergo extra divisions and elongate.

Discussion

MS32 controls a division/differentiation switch in anther cell layer development

As an anther develops from a stamen primordium, it goes through a series of cell divisions and differentiation. Divisions in the epidermis are solely anticlinal, and are required for growth in anther length and girth (Kelliher and Walbot, 2011). The internal layers, however, undergo a well controlled series of division and differentiation events. The L2-derived cells internal to the epidermis show random division planes before the archesporial cells are specified (Kelliher and Walbot, 2011). This disorganized pattern closely resembles the core of a shoot apical meristem where pluripotent stem cells reside. Possibly, the L2-derived cells at this early stage have some stem cell-like characteristics, thus allowing the archesporial cells to arise from its population (Kelliher and Walbot, 2011). Concurrently with the germ cell specification in each anther lobe, the surrounding somatic cells become organized into a dartboard pattern with the archesporial cells in the center. The first periclinal division in the L2-derived somatic cells results in an anther with three somatic layers, and soon after this division, the subepidermal layer differentiates into the endothecium (Figures 1b and 2a). The inner layer, called the secondary parietal layer, still remains undifferentiated. After a period of anticlinal cell divisions, the second periclinal division occurs in the secondary parietal layer to form a four-layered anther wall (Figures 1b and 2b). The two newly formed layers differentiate into the middle layer and the tapetum (Figures 1b and 2c). Once established, these two layers strictly divide only anticlinally. Thus, there likely is a control mechanism in place to shut off further periclinal divisions in differentiated cells.

The extra periclinal divisions in the *ms32-ref* anther wall suggest that *ms32* controls a switch required to inhibit extra periclinal divisions in differentiated somatic layers. If *ms32* was the only regulator for this process, all somatic layers should display additional divisions to a similar degree. What is observed is that tapetal cell precursors are most heavily affected by the absence of MS32, followed by the presumptive middle layer and more rarely the endothecial cells (Figures 2 and S1; Chaubal *et al.*, 2000). This layer in *ms32-ref* fails to acquire tapetal cell characteristics, such as dense cytoplasm or binucleate cell formation (Figure 1d; Chaubal *et al.*, 2000). We hypothesize that the absence of MS32 function causes the presumptive tapetal precursors to get stuck in an undifferentiated state that resembled its secondary parietal layer precursor, thus resulting in the failure to inhibit further periclinal divisions. In the other somatic layers, signals to stop periclinal divisions have to be programmed by other factors that can participate in regulation of periclinal division. Without a functional *ms32*, suppression of periclinal division is incomplete, and allowed some cells to escape from this control and undergo an additional round of periclinal division (Figure 7).

The extra division phenotype of *ms32-ref* becomes even more severe in the double mutant with *mac1-1*. In *mac1* mutants, the very first periclinal division in the L2-derived cells is defective, a result that suggested a role of MAC1 in promoting this division (Wang *et al.*, 2012). The undifferentiated L2-derived cells in *ms32-ref mac1-1* keep dividing, this situation probably reflects the absence of functional MS32, which resulted in many small cells filling up the anther lobes (Figure 5h). Likely, MAC1 is secreted by the archesporial cells and leads to a gradient of MAC1 that is important for setting up the dartboard organization of the anther somatic layers (Wang *et al.*, 2012). Without functional MAC1 in *ms32-ref mac1-1*, the anther lobes are missing this guidance cue to establish the division planes, leading to a disorganized pattern of cells (Figure 5h).

Among the previously identified male sterile mutants, the gene products of *ms23-SB131*, *ems72091*, *tcl1*, *mtm00-06* and *ocl4* serve as good candidates to be involved in inhibition of periclinal division in differentiated cells (Chaubal *et al.*, 2000; Vernoud *et al.*, 2009; Timofejeva *et al.*, 2013). Unlike *ms32-ref*, the *ms23-SB131* mutant allows one single additional periclinal division in the innermost anther wall layer (presumptive tapetal cells), and formed two identical layers of undifferentiated precursor cells (Chaubal *et al.*, 2000). Thus these two mutants differ substantially in their defects: *ms23* could be interpreted as a tapetal precursor repeating the SPL periclinal division program precisely, while *ms32* shows many ectopic periclinal divisions over an extended time frame and in multiple cell types. Both *tcl1* and *mtm00-06* exhibit extra periclinal divisions in the SPL or its immediate derivatives and the *ems72091* mutant is unique in that the periclinal division is mis-regulated only in the middle layer (Timofejeva *et al.*, 2013). Cytological characterization suggests that the four layers are formed properly then the periclinal division occurs in the middle layer, and indicated that this gene product is required to maintain the middle layer in its differentiated state and to prevent additional periclinal divisions from happening. The *ocl4* mutant, on the other hand, has an extra layer of endothecium (Vernoud *et al.*, 2009). Interestingly, the differentiation of the endothecium occurs properly, this situation suggests that the HD-ZIP IV transcription factor, OCL4, function is not required for endothecium differentiation but is restricted to inhibition of extra periclinal divisions in the subepidermal

layer. This model for OCL4 function is further supported by the *ocl4 mac1-1* double mutant, which shows an additive phenotype with an extra subepidermal layer in anther lobe with an overall *mac1*-like phenotype (Wang *et al.*, 2012). That future cloning of these additional genes affects periclinal division control and should help to elucidate the mechanisms that underlie periclinal division control, in particular cell types during anther development.

Unique role of MS32 in anther development

The *ms32* gene encodes a bHLH protein, which possibly functions as a transcription factor (Figure 3). Analysis based on synteny and sequence similarity suggests that MS32 is an ortholog of the rice UDT1 protein (Figures S3 and S4), which also regulates anther development (Jung *et al.*, 2005). The phenotype of *udt1-1* differs from *ms32-ref* in that the middle layer and tapetum are differentiated normally in *udt1-1* and extra periclinal divisions are not observed (Jung *et al.*, 2005). The tapetal cells, however, become highly vacuolated as the anther matures. Another phenotypic distinction is that in *ms32-ref*, pollen mother cells fail to complete meiotic prophase I and are squashed by the extra somatic cell layers (Chaubal *et al.*, 2000; Timofejeva *et al.*, 2013). In contrast, meiosis in *udt1-1* anthers can proceed to the dyad stage followed by tetrad degeneration (Jung *et al.*, 2005). The phenotype of *udt1* closely relates to the phenotype of the Arabidopsis mutant defective in *DYSFUNCTIONAL TAPETUM1* (*DYT1*), which also encodes a bHLH protein (Zhang *et al.*, 2006). The Arabidopsis ABORTED MICROSPORES (AMS) is another bHLH protein that is known to function downstream of DYT1 (Sorensen *et al.*, 2003; Xu *et al.*, 2010; Ma *et al.*, 2012). Phylogenic analyses of UDT1, DYT1, and AMS1 with other bHLH proteins have shown that they group together, within which UDT1 forms a clade with DYT1 (Zhang *et al.*, 2006). Despite the close relationship among these proteins, the extra periclinal divisions observed in *ms32-ref* are not found in rice and Arabidopsis and suggested that MS32 is unique in its function to regulate periclinal divisions.

Consistent with its proposed role, *ms32* expression is temporally restricted to the pre-meiotic anther (Figure 3). While its early expression initiates broadly, expression is spatially restricted to the secondary parietal layer and the tapetum layer as the anther develops (Figure 4). This expression pattern coincides with the proposed function in control of division and differentiation in these layers. As shown for other bHLH proteins, it is likely that MS32 forms homo- or heterodimers with other bHLH proteins (Nair and Burley, 2000; Toledo-Ortiz *et al.*, 2003; Carretero-Paulet *et al.*, 2010). The DYT1 and AMS protein in Arabidopsis interact with other bHLH proteins, forming a complex gene regulatory network during anther development (Xu *et al.*, 2010; Ma *et al.*, 2012). The binding site of DYT1 has been characterized and its function as a transcriptional activator has been proposed (Feng *et al.*, 2012). The *ms32-6066* allele, with two amino acid insertion in the bHLH domain, will serve as an excellent starting point to further understand the molecular basis of this protein–protein interaction and the *in vivo* function as a transcriptional activator. The two amino acid insertion resides in the loop subdomain of the bHLH domain, a variable region that separates the two helices. However, studies have shown that the loop region can affect the DNA binding affinity of the protein dramatically (Nair and Burley, 2000; Winston and Gottesfeld, 2000). Perhaps the two amino acids inserted in the *ms32-6066* mutant protein disrupt its binding to DNA, which makes it functionally defective. Future work to identify MS32-

interacting partners and analysis of the mutant MS32 protein in various allelic combinations of homo and heterodimers, will be useful in the understanding of the molecular mechanism of MS32 protein function.

Experimental Procedures

Plant material

The *ms32-ref* mutant was previously reported to be derived from Robertson's Mutator maize lines (Chaubal *et al.*, 2000). The *ms32-6066* allele was obtained from the Maize Genetics Cooperation Stock Center (http://maizecoop.cropsci.uiuc.edu) under the name of *ms*6066* (Timofejeva *et al.*, 2013). The two Uniform*Mu* lines (Settles *et al.*, 2007; McCarty and Meeley, 2009), *mu1043594::Mu* (UF*Mu*-05337) and *mu1019067::Mu* (UF*Mu*-00626) were also from the Maize Genetics Cooperation Stock Center. *mac1-1* has been described previously in Wang *et al*. (2012).

Histological analysis

Spikelets were dissected from each plant and fixed in 3:1 ethanol: acetic acid. After dehydration through an ethanol series, spikelets were embedded into low viscosity Spurr's epoxy resin (Electron Microscopy Sciences Catalog #14300, http://www.emsdiasum.com/microscopy). Next, 0.5-μm semi-thin sections were obtained using a Reichert Ultracut E microtome (Reichert, http://www.reichert.com) and stained with 0.1% Toluidine Blue O and observed in bright field.

Positional cloning

ms32 was previously mapped to chromosome 2 (Chaubal *et al.*, 2000). A series of bulked segregant analyses was conducted to finely map and clone *ms32*. Initial mapping was conducted using a set of 22 insertion-deletion primer pairs spaced approximately 10 cM apart and tested against gDNA pools of eight male-fertile and nine male sterile individuals from a 1:1 segregated population. Primer pair IDP792 on chromosome 2 (map position 136.1) showed polymorphism between the male-fertile and male sterile gDNA pools. An additional BSA experiment was conducted using a set of 24 IDP primer pairs that span map positions 112.3–153.1 on chromosome 2. Polymorphic primer pairs within this interval were identified and used to map breakpoints in recombinant individuals from the initial set of 17 plants. A larger mapping population consisting of 249 male sterile individuals was generated and analyzed, and the candidate gene interval was narrowed to approximately 0.5 Mb on chromosome 2 between *umc1049* and a custom developed marker, JM16 (5′-GGGCTACGTCGACAGCC CTC-3′ and 5′-CTCAACCAATCATGCCACGAC-3′) at 201.94 Mb.

RNA isolation and expression analysis

Total RNA was purified using Trizol reagent (Invitrogen, http://www.lifetechnologies.com/us/en/home/brands/invitrogen.html) in accordance with the manufacturer's instructions. RNA (1 μg) from each sample was reverse-transcribed using Superscript III (Invitrogen). Quantitative PCR (qPCR) was performed on an Applied Biosystems 7300 Real-Time PCR system (http://www.appliedbiosystems.com/absite/us/en/

home.html) using Fast Plus EvaGreen qPCR Master Mix–High Rox (Biotium, http://www.biotium.com/). Data were averages from at least three qRT-PCR replicates and normalized against *gapdh* or *cyanase* levels. Sequences of primers used are as follows: *gapdh*, ZmGAPDH-5F, 5′-CCTGCTTCTCA TGGATGGTT-3′; and ZmGAPDH-6R, 5′-TGGTAGCAGGAAGGGA AACA-3′; *cyanase*, Cyanase-F, 5′-GCTGGTGAGGAGGAGAAACA-3′ and Cyanase-R, 5′-CAGCAATCATGCCAGGTAGA-3′; *ms32* exon 1 and 2, JM20-F, 5′-ATGCCGCGCCGGCGGAGGAC-3′ and JM21-R, 5′-CTGATACGGCATGTTTTCCG-3′; *ms32* exon 3 and 4, JM55-F, 5′-GGTCAGATCGAGCTGGTTCCT-3′ and JM20-R, 5′-TCAGTTGCTT GGGACCTCCA-3′. Whole length cDNA was amplified using primers JM20-F and JM20-R.

In situ hybridization

Immature tassels of 3–5 cm were fixed overnight with 50% ethanol, 5% glacial acetic acid, 3.7% formaldehyde, 0.5% Triton X-100, and 1% dimethyl sulfoxide. Samples were dehydrated through ethanol series and stained with 0.5% (w/v) Eosin Y in ethanol, which were followed by paraffin embedding. For *in situ* hybridization of *ms32*, tissue sections were pre-treated and hybridized as described previously (Jackson *et al.*, 1994). The template for the antisense *ms32* probe was amplified using JM55-F and JM20-R, described above.

Supplementary Material

Refer to Web version on PubMed Central for supplementary material.

Acknowledgments

This work was supported by NSF grant DBI-0701880 to V.W and W.Z.C. We would like to thank Lisa Harper and Sarah Hake for their critical reading of the manuscript.

References

Albertsen, MC.; Fox, T.; Trimnell, M.; Wu, Y. *MSCA1* nucleotide sequences impacting plant male fertility and method of using same. U.S. patent 7915478. 2011.

Carretero-Paulet L, Galstyan A, Roig-Villanova I, Martinez-Garcia JF, Bilbao-Castro JR, Robertson DL. Genome-wide classification and evolutionary analysis of the bHLH family of transcription factors in Arabidopsis, poplar, rice, moss, and algae. Plant Physiol. 2010; 153:1398–1412. [PubMed: 20472752]

Chaubal R, Zanella C, Trimnell MR, Fox TW, Albertsen MC, Bedinger P. Two male-sterile mutants of *Zea mays* (Poaceae) with an extra cell division in the anther wall. Am J Bot. 2000; 87:1193–1201. [PubMed: 10948005]

Chaubal R, Anderson JR, Trimnell MR, Fox TW, Albertsen MC, Bedinger P. The transformation of anthers in the *msca1* mutant of maize. Planta. 2003; 216:778–788. [PubMed: 12624765]

Dawe RK, Freeling M. Clonal analysis of the cell lineages in the male flower of maize. Dev Biol. 1990; 142:233–245. [PubMed: 2172058]

Feng B, Lu D, Ma X, Peng Y, Sun Y, Ning G, Ma H. Regulation of the Arabidopsis anther transcriptome by DYT1 for pollen development. Plant J. 2012; 72:612–624. [PubMed: 22775442]

Jackson D, Veit B, Hake S. Expression of maize KNOTTED1 related homeobox genes in the shoot apical meristem predicts patterns of morphogenesis in the vegetative shoot. Development. 1994; 120:405–413.

Jung KH, Han MJ, Lee YS, Kim YW, Hwang I, Kim MJ, Kim YK, Nahm BH, An G. Rice *Undeveloped Tapetum 1* is a major regulator of early tapetum development. Plant Cell. 2005; 17:2705–2722. [PubMed: 16141453]

Kelliher T, Walbot V. Emergence and patterning of the five cell types of the *Zea mays* anther locule. Dev Biol. 2011; 350:32–49. [PubMed: 21070762]

Kelliher T, Walbot V. Hypoxia triggers meiotic fate acquisition in maize. Science. 2012; 337:345–348. [PubMed: 22822150]

Lyons E, Freeling M. How to usefully compare homologous plant genes and chromosomes as DNA sequences. Plant J. 2008; 53:661–673. [PubMed: 18269575]

Lyons E, Pedersen B, Kane J, et al. Finding and comparing syntenic regions among Arabidopsis and the outgroups papaya, poplar, and grape: CoGe with rosids. Plant Physiol. 2008; 148:1772–1781. [PubMed: 18952863]

Ma H. Molecular genetic analyses of microsporogenesis and microgametogenesis in flowering plants. Annu Rev Plant Biol. 2005; 56:393–434. [PubMed: 15862102]

Ma X, Feng B, Ma H. AMS-dependent and independent regulation of anther transcriptome and comparison with those affected by other Arabidopsis anther genes. BMC Plant Biol. 2012; 12:23. [PubMed: 22336428]

McCarty, DR.; Meeley, RB. Transposon resources for forward and reverse genetics in maize. In: Bennetzen, JL.; Hake, S., editors. Maize Handbook – Volume II: Genetics and Genomics. London: Springer; 2009. p. 561-584.

Nair SK, Burley SK. Recognizing DNA in the library. Nature. 2000; 404:715–718. [PubMed: 10783871]

Nonomura KI, Miyoshi K, Eiguchi M, Suzuki T, Miyao A, Hirochika H, Kurata N. The *MSP1* gene is necessary to restrict the number of cells entering into male and female sporogenesis and to initiate anther wall formation in rice. Plant Cell. 2003; 15:1728–1739. [PubMed: 12897248]

Settles AM, Holding DR, Tan B, et al. Sequence-indexed mutations in maize using the Uniform*Mu* transposon-tagging population. BMC Genomics. 2007; 8:116. [PubMed: 17490480]

Sheridan WF, Golubeva EA, Abrhamova LI, Golubovskaya IN. The *mac1* mutation alters the developmental fate of the hypodermal cells and their cellular progeny in the maize anther. Genetics. 1999; 153:933–941. [PubMed: 10511568]

Sorensen AM, Kröber S, Unte US, Huijser P, Dekker K, Saedler H. The Arabidopsis *ABORTED MICROSPORES* (*AMS*) gene encodes a MYC class transcription factor. Plant J. 2003; 33:413–423. [PubMed: 12535353]

Timofejeva L, Skibbe DS, Lee S, Golubovskaya I, Wang R, Harper L, Walbot V, Cande WZ. Cytological characterization and allelism testing of anther developmental mutants identified in a screen of maize male sterile lines. G3 (Bethesda). 2013; 3:231–249. [PubMed: 23390600]

Toledo-Ortiz G, Huq E, Quail PH. The Arabidopsis basic/helix--loop-helix transcription factor family. Plant Cell. 2003; 15:1749–1770. [PubMed: 12897250]

Vernoud V, Laigle G, Rozier F, Meeley RB, Perez P, Rogowsky PM. The HD-ZIP IV transcription factor OCL4 is necessary for trichome patterning and anther development in maize. Plant J. 2009; 59:883–894. [PubMed: 19453441]

Wang CJR, Nan GL, Kelliher T, et al. Maize *multiple archesporial cells 1* (*mac1*), an ortholog of rice TDL1A, modulates cell proliferation and identity in early anther development. Development. 2012; 139:2594–2603. [PubMed: 22696296]

Winston RL, Gottesfeld JM. Rapid identification of key amino-acid-DNA contacts through combinatorial peptide synthesis. Chem Biol. 2000; 7:245–251. [PubMed: 10780928]

Xu J, Yang C, Yuan Z, Zhang D, Gondwe MY, Ding Z, Liang W, Zhang D, Wilson ZA. The ABORTED MICROSPORES regulatory network is required for postmeiotic male reproductive development in Arabidopsis thaliana. Plant Cell. 2010; 22:91–107. [PubMed: 20118226]

Zhang W, Sun Y, Timofejeva L, Chen C, Grossniklaus U, Ma H. Regulation of Arabidopsis tapetum development and function by *DYSFUNCTIONAL TAPETUM1* (*DYT1*) encoding a putative bHLH transcription factor. Development. 2006; 133:3085–3095. [PubMed: 16831835]

Zhao X, de Palma J, Oane R, Gamuyao R, Luo M, Chaudhury A, Hervé P, Xue Q, Bennett J. OsTDL1A binds to the LRR domain of rice receptor kinase MSP1, and is required to limit sporocyte numbers. Plant J. 2008; 54:375–387. [PubMed: 18248596]

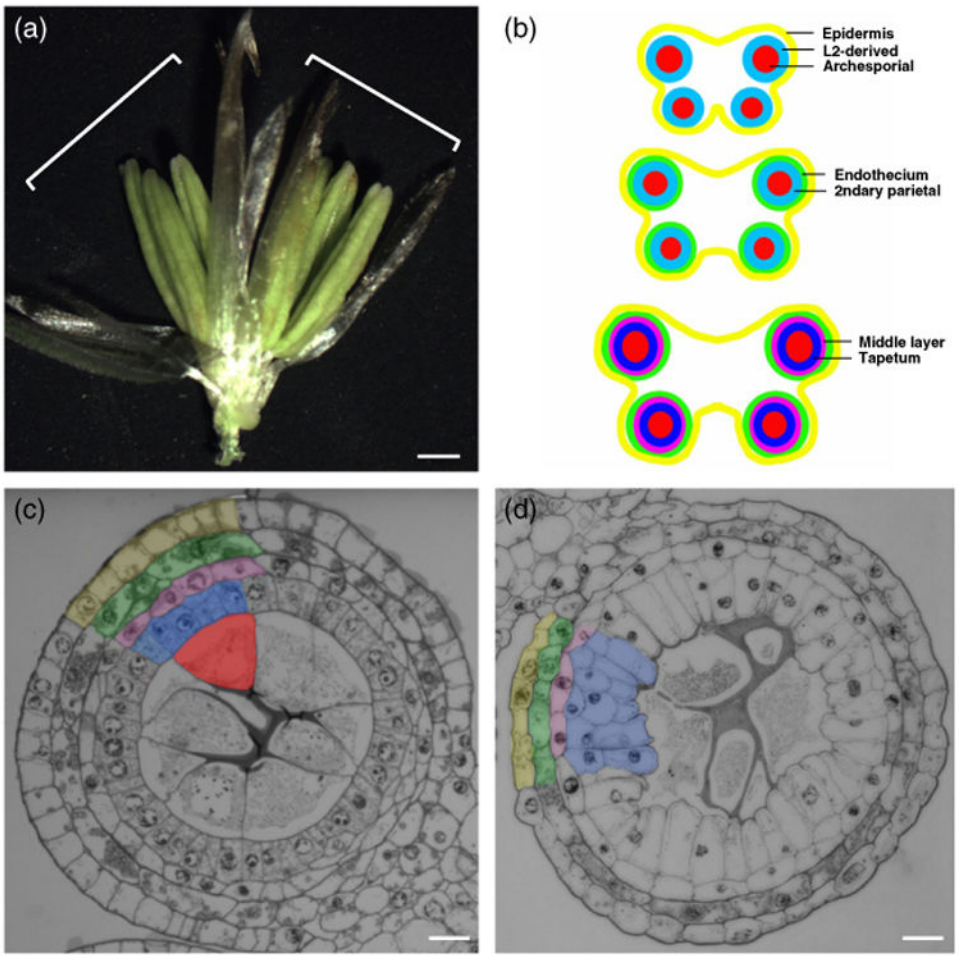

Figure 1.

Anther development in maize.

(a) Maize spikelet showing the two florets (white brackets) with three anthers each. Scale bar: 1 mm.

(b) Schematic drawing of anther development in maize.

(c, d) Transverse section of fertile (c) and *ms32-ref* (d) anthers. Layers in (c) are color coded as in (b). Same colors are used for the middle layer and tapetal precursor cells in (d). Scale bars: 20 μm.

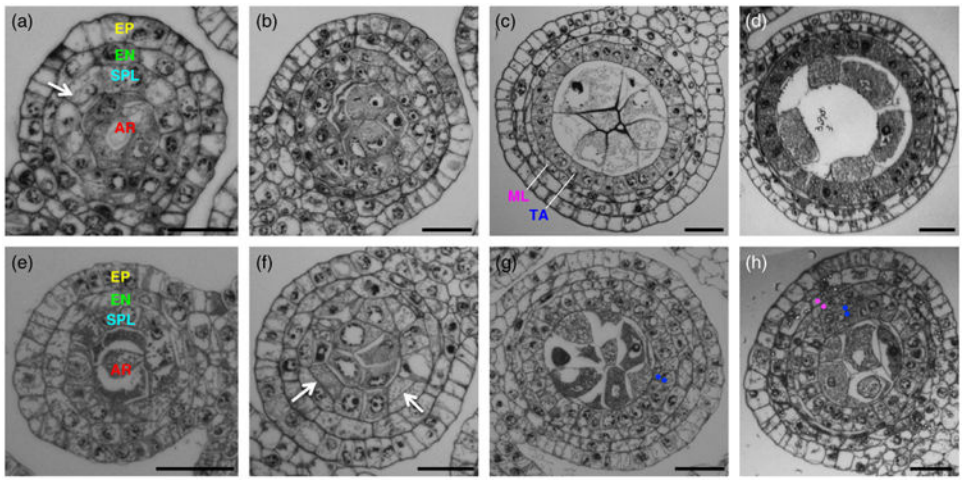

Figure 2.

Defects of *ms32-ref* initiate after the four somatic layers are formed. Transverse sections of developing wild-type (a–d) *and ms32-ref* (e–h) anthers are shown.

(a, e) Both wild-type (a) and mutant (e) anthers with three somatic layers are shown.

(b, f) The layer that surrounds the archesporial cells (secondary parietal cells) divides periclinally (white arrows in (a) and (f)) to form four somatic layers in both wild-type (b) and mutant (f).

(c, g) Fertile and mutant anthers with four somatic layers are shown. Differentiation occurs in the middle layer and the tapetum of a wild-type anther (c) leading to differences in cytoplasmic densities and cell sizes. In the mutant anther (g), the tapetal precursor cells fail to obtain the tapetal characteristics and extra divisions occur (white dots).

(d, h) Later stage anthers of wild-type (d) and mutant (h) clearly show the defects of *ms32-ref* with extra divisions and undifferentiated cells. Magenta-colored dots indicate extra divisions in the middle layer, while blue dots indicate extra divisions in the tapetum. Layers are color coded as in Figure 1. AR, archesporial; EN, endothecium; EP, epidermis; ML, middle layer; SPL, secondary parietal layer; TA, tapetum. Scale bars: 20 μm.

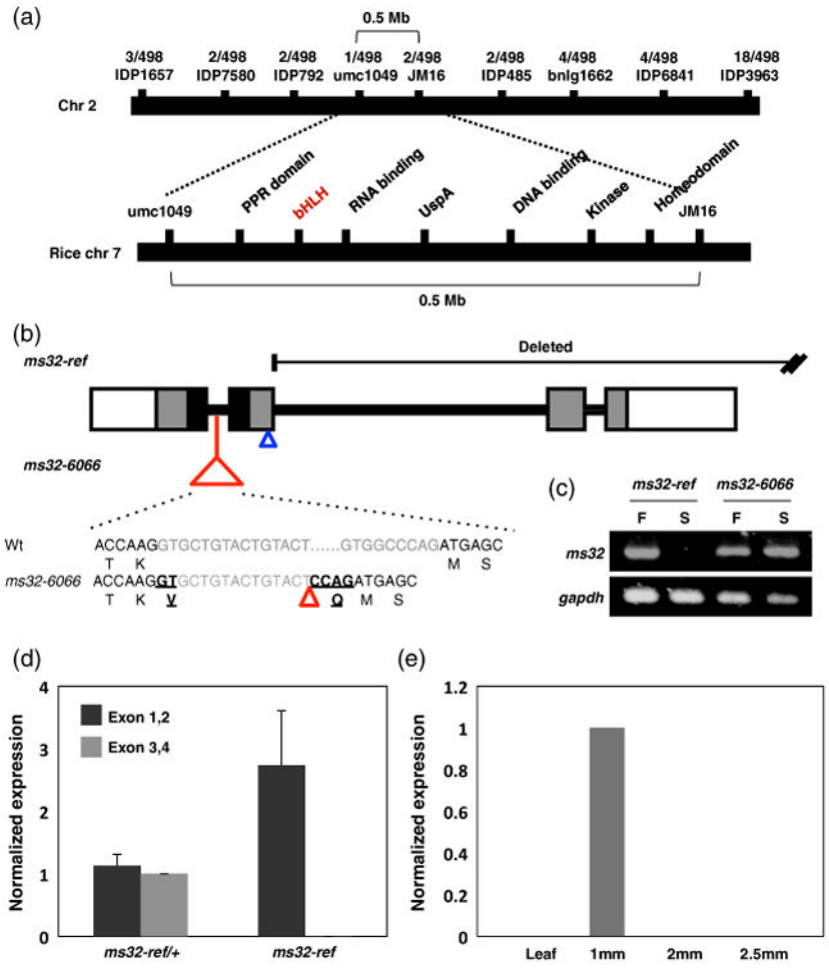

Figure 3.

Positional cloning of the *ms32* gene.

(a) The *ms32* gene was mapped to a 0.5 Mb interval on chromosome 2. This region is syntenic to rice chromosome 7.

(b) The gene structure of *ms32* with four exons (in grey boxes) and three introns (black lines). The black box marks the bHLH domain while the white boxes indicate the 5′ and 3′ UTRs. The *ruq*-transposon insertion in *ms32-6066* is shown as a red triangle. The black sequences denote the exons while the gray letters correspond to the intron sequence of wild-type and *ms32-6066*. The translation is shown below the nucleotide sequence. The six nucleotide insertion caused by the mis-splicing of the *ruq*-transposon is indicated by underlining. The position of *mu1043594*::*Mu* is shown with a blue triangle.

(c) PCR amplification of the protein coding region from wild-type, *ms32-ref* and *ms32-6066*. Amplification failed in the *ms32-ref* but exists in *ms32-6066*. F, fertile; S, sterile siblings.

(d) qRT-PCR of *ms32* with two different primers. Black bars show the result using primers specific to exon 1, 2, while the grey bars show the result using primers against exon 3, 4.

(e) Expression analysis of *ms32* indicates specific expression in pre-meiotic anthers. Error bars indicate standard deviation values.

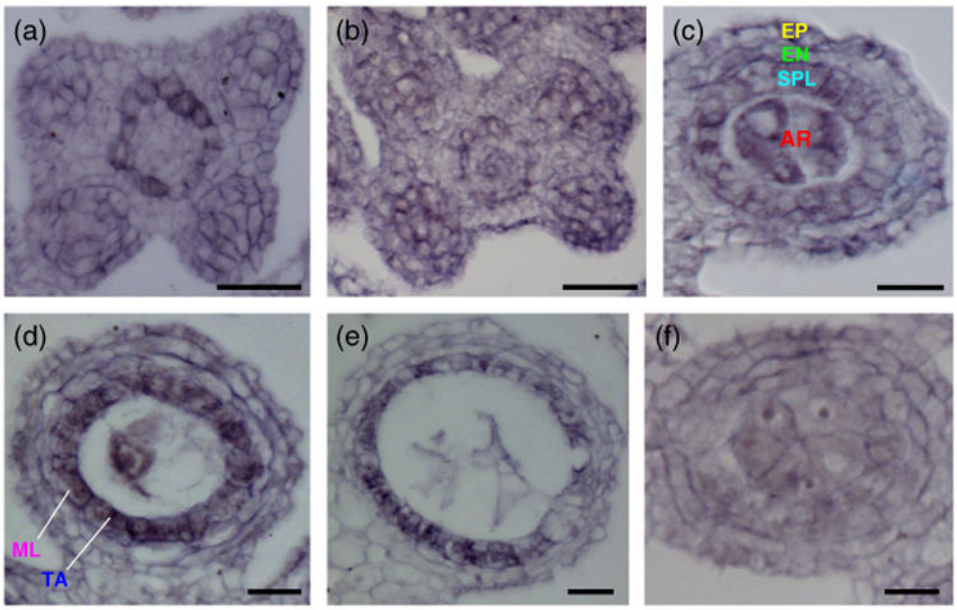

Figure 4.

ms32 expression in developing anthers.

(a–f) Transverse sections of wild-type anthers.

(a, b) *ms32* is expressed broadly in the four lobes and the cells that surround the central vasculature in premature anthers prior (a) and after (b) archesporial cell specification.

(c, d) *ms32* expression becomes restricted to the secondary parietal layer (c) and the tapetal precursors (d) as the anther develops. Expression is also detected in the central archesporial cells.

(e) After differentiation of all somatic layers, *ms32* expression persists in the tapetum and becomes weaker in the pollen mother cells.

(f) No specific expression is observed in the *ms32-ref* mutant. Layers are color coded as in Figure 1. AR, archesporial; SPL, secondary parietal layer; EN, endothecium; EP, epidermis; ML, middle layer; TA, tapetum. Scale bars: 20 μm.

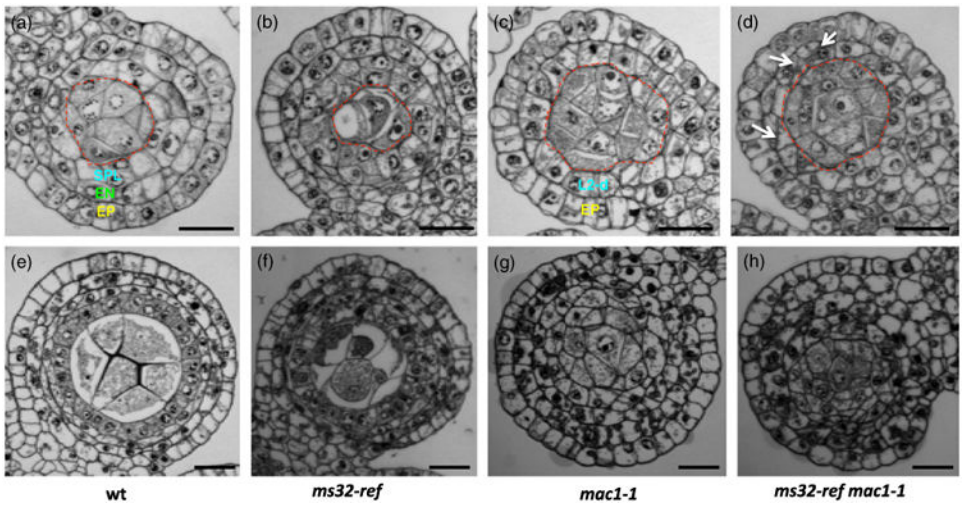

Figure 5.

ms32-ref enhances the *mac1-1* phenotype.

(a–h) Transverse sections of wild-type (a, e), *ms32-ref* (b, f), *mac1-1* (c, g) and *ms32-ref mac1-1* (d, h) anthers.

(a–d) Wild-type (a) and *ms32-ref* (b) are anthers that are undergoing periclinal division in the secondary parietal layer. At the same stage, *mac1-1* (c) and *ms32-ref mac1-1* (d) retain just two somatic layers, the epidermis and the L2-derived layer. Additional divisions (indicated by white arrows) are observed in some L2-derived cells of *ms32-ref mac1-1* anther lobes. Archesporial cells (marked by the red dotted lines) are numerous in both *mac1-1* and *ms32-ref mac1-1*.

(e–h) Anther lobes at a later stage. In wild-type (e), four somatic layers surround the pollen mother cells and differentiation occurs, while *ms32-ref* (f) shows four layers with excess divisions and failure of differentiation. Both *mac1-1* (g) and *ms32-ref mac1-1* (h) have disorganized cell layers, however, smaller cells were observed in the double mutant. Layers are color coded as in Figure 1. AR, archesporial; EN, endothecium; EP, epidermis; SPL, secondary parietal layer. Scale bars: 20 μm.

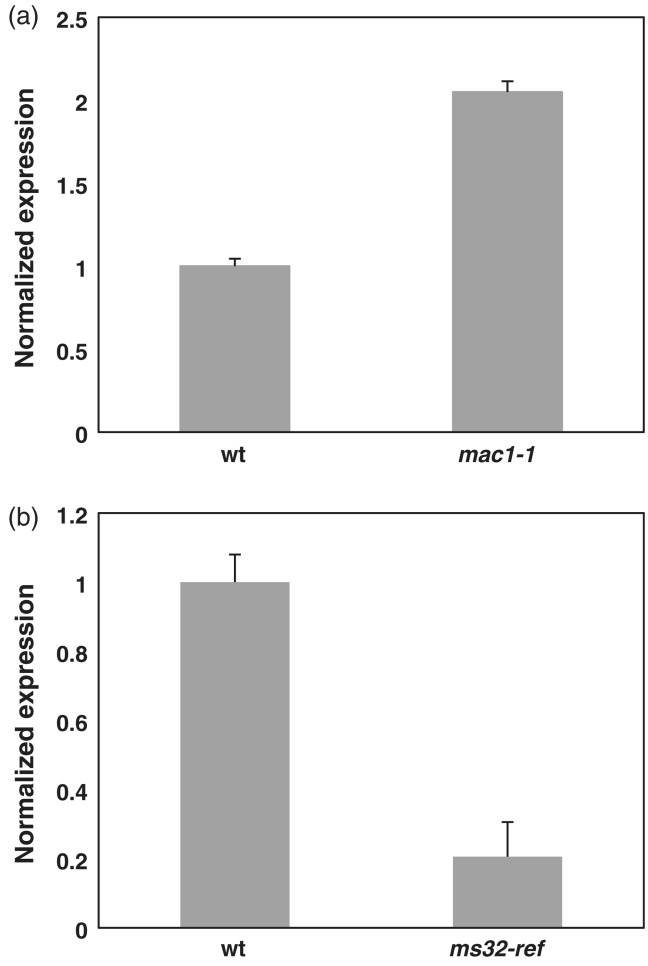

Figure 6.

ms32 and *mac1* expression are reciprocally altered by the *mac1-1* and *ms32-ref* mutations.

(a) qRT-PCR results show *ms32* expression in *mac1-1*.

(b) qRT-PCR results show *mac1* expression in *ms32-ref*. Mixed stages of anthers were used to cover the whole developmental period. Error bars indicate values for standard deviation.

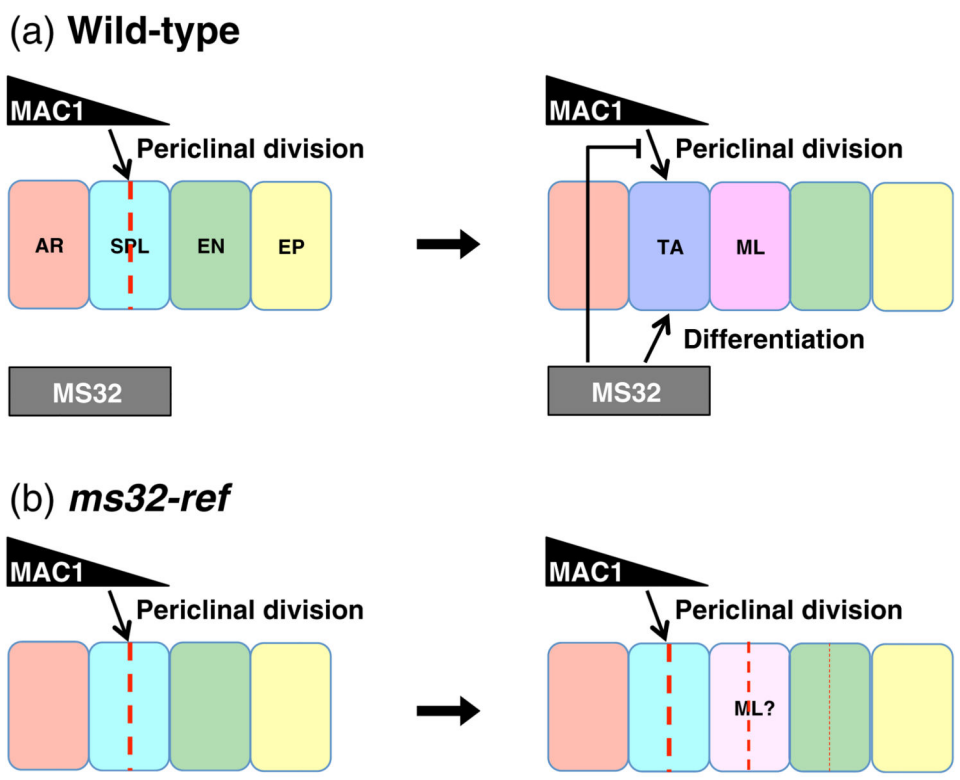

Figure 7.
Model for MS32 function.

(a) In wild-type, MAC1 secreted by the archesporial cells has a demonstrated role in promoting periclinal division of L2-derived cells and we propose that it similarly promotes periclinal division in the secondary parietal layer. Once these periclinal divisions complete in the secondary parietal layer, MS32 promotes differentiation in the most inner layer, which normally becomes the tapetum. Concurrently, MS32 inhibits further periclinal division in the differentiated layers.

(b) In *ms32-ref*, periclinal division is normal and four somatic layers form. Without a functional MS32, differentiation of the tapetum fails and additional periclinal divisions occur in this layer. Less frequently, the middle layer and the endothecium exhibit extra periclinal divisions. The frequency of periclinal divisions are shown by differences in thickness of the red dotted lines. AR, archesporial cells; EP, epidermis; EN, endothecium; ML, middle layer; SPL, secondary parietal layer; TA, tapetum.